ELSEVIER

PII: S0032-3861(97)00596-X

Polymer Vol. 39 No. 13, pp. 2769–2775, 1998

0032-3861/98/$19.00+0.00

Time-resolved light scattering study on the gelation process of poly(*N*-isopropyl acrylamide)

Tomohisa Norisuye, Mitsuhiro Shibayama* and Shunji Nomura
Department of Polymer Science and Engineering, Matsugasaki, Sakyo-kuKyoto 606 Japan
(Received 2 May 1997; revised 9 July 1997; accepted 17 July 1997)

The generation process of poly(*N*-isopropyl acrylamide) (PNIPA) gels has been studied by time-resolved light scattering. The gelation was initiated by adding a redox initiator and cross-linker (*N,N'*-methylenebisacrylamide, BIS). The scattered intensity was observed at a fixed angle of 60° as a function of polymerization/gelation time, t. The scattered intensity had an abrupt rise at $t \approx 20$ min, then reached a plateau value having relatively large fluctuations. In the case of the corresponding PNIPA solutions, prepared without BIS, similar behaviour was observed, although the pulse height and the plateau intensities were significantly lower. In both cases, the abrupt intensity rise disappeared when the monomer concentration, C, was reduced to 88 mM or lower. In addition, a gel was not formed for $C \leq 88$ mM even in the presence of BIS. It was concluded by viscometry and the monomer concentration dependence experiment that (i) the abrupt intensity rise corresponds to the gelation threshold and (ii) and so-called chain overlap concentration can be estimated by the appearance of the abrupt intensity rise (in this particular case, $88 \leq C^* \leq 131$ mM). The abrupt rise in the scattered intensity was also observed by small-angle neutron scattering, suggesting that the gelation threshold can be observed in a wide range of momentum transfer space.

(Keywords: time-resolved light scattering; poly(*N*-isopropyl acrylamide); gelation)

INTRODUCTION

Gelation, i.e. the sol–gel transition, of polymers, has been the object of study for more than a half century. In the 1940s, Flory discussed the criterion of infinite cluster formation of polymer chains by polycondensation of two- and three-functional monomer mixtures[1–3]. The classical picture of gelation on the basis of the Bethe lattice is given by Stockmayer[4,5]. A scaling theory of the gelation was developed by Stauffer[6], and the critical phenomenon of gelation was discussed by Stauffer et al. on the basis of percolation theory[7]. Experimental studies on gelation have been conducted by light scattering[8,9], small-angle X-ray scattering[10], and small-angle neutron scattering[11], where the growth of polymer chain clusters was terminated just below the gelation threshold and the cluster solution was diluted in order to detect the single-cluster scattering. Mechanical and rheological measurements allow one to perform an in situ measurement of the gelation process[7]. These developments in the study of gelation are reviewed concisely in the textbook by de Gennes[12].

Recently, Winter and coworkers proposed a novel method to determine the gelation point with an oscillatory shear experiment. According to their theory, the storage, $G'(\omega)$, and loss moduli, $G''(\omega)$, becomes equal and scale to $\omega^{1/2}$, at the gelation point, i.e. $G'(\omega) = G''(\omega) \sim \omega^{1/2}$, where ω is the angular frequency[13,14]. Its validity was examined by the cross-linking process of polydimethylsiloxane[14] and dihydroxypoly(propylene oxide) (model polyurethane)[15], etc. In the case of light scattering, on the other hand, an in situ (or real time) determination of the gelation threshold has been thought to be difficult because scattering signals in a gelling solution are dominated by interference between different clusters and are weak[12]. However, some studies have been carried out in a reaction bath. Kobayasi introduced a method to detect the gelation point of a gelatin solution. Polystyrene latex particles were dispersed in a gelatin solution and the scattered light intensity was measured as a function of the scattering angle. The gelation point was detected as the appearance of a speckle pattern due to immobilization of the latex particles[16]. A similar method was reported by Allain et al. for acrylamide gels[17]. Fang et al. however, reported that dynamic light scattering is sensitive to the sol–gel transition of polymer solutions by chemical cross-linking[19]. They observed a critical behaviour in the dynamics near the sol–gel transition, which is characterized by a presence of a power-law type spectrum for the time intensity correlation function. Therefore, an appearance of non-exponential decay in the correlation function indicates the sol–gel transition. Similar behaviour was observed by Ikkai et al[20].

We have found that a simpler experiment, monitoring light scattered intensity as a function of time, i.e. the time-resolved light scattered (TRLS) intensity measurement at a fixed angle, allows one to monitor quite easily the cluster evolution process with time and to determine the gelation threshold for poly(acrylamide) and poly(*N*-isopropylacrylamide) aqueous gels. Although this method is similar to the one employed by Wu et al.[18] in a curing process of epoxy resins, we emphasize the following in this paper: (1) The time course of the scattered intensity shows characteristic

* To whom correspondence should be addressed

patterns that depend on the architecture of the polymers, such as linear polymer solutions or cross-linked gels. (2) The so-called chain overlap concentration is also detectable by a series of TRLS experiments with different monomer concentrations. (3) This method is useful to study the gelation kinetics not only of the gelling system from a monomer solution but also from a cross-linking of polymer solutions.

EXPERIMENTAL SECTION

Sample preparation

Poly(*N*-isopropyl acrylamide) (PNIPA) gels and the corresponding polymer solutions were prepared by redox polymerization. NIPA monomers, supplied by Kohjin Chemical Co., were purified by recrystallization prior to the use. NIPA monomer concentrations were varied from 48, to 801 mM (8 concentrations), while the *N,N'*-methylenebisacrylamide (BIS, cross-linker) concentration was fixed to be 8.62 mM (for the gels) and 0 mM (for the corresponding PNIPA solutions). After adding 1.75 mM of ammonium persulphate (APS; initiator), the monomer solution was degassed for 15 min with a vacuum pump and cooled in a refrigerator for another 15 min in order to decelerate the polymerization reaction. Then, 8 mM of *N,N,N',N'*-tetramethylethylenediamine (TMEDA, accelerator) was added to the system, and the monomer solution was filtered with a 0.2 μm filter before polymerization. The polymerization was performed in a 10 mm-diameter test tube at 25°C. Reagent grade BIS and APS were purchased from Wakenyaku Co. Ltd. and were used without further purification.

Light scattering

Light scattering (LS) experiments were conducted on a custom-built light-scattering apparatus with a 10 mW He–Ne laser and a photon correlator (DLS-7, Otsuka Electric. Co.). For time-resolved LS (TRLS) experiments, the scattering angle was fixed at 60° unless stated and more than 12 000 intensity data values were collected as a function of the polymerization time, t, during about 2 hours of reaction. Dynamic light-scattering experiments were also carried out for samples after completion of gelation.

Small-angle neutron scattering

Time-resolved small-angle neutron scattering experiments were carried out on the reactor, SANS-U, at Institute of Solid State Physics, The University of Tokyo, located at Japan Atomic Energy Laboratories, Tokai, Japan. A flux of cold neutrons of 7 Å was irradiated onto the gelling sample in deuterated water, and the scattered intensity was collected every 5 min with an area detector of 128 × 128 pixels. The sample-to-detector distance was set to be 4 m. The sample was placed in a brass chamber with quartz windows and the chamber was thermo-regulated within an error of ± 0.5°C at the sample position with a NESLAB 110 water circulating bath. The sample thickness was about 1.5 mm.

Viscometry

The viscosity of the PNIPA solutions was measured with a Ubbelohde capillary viscometer at 25 ± 0.1°C. The measurements were repeated at least three times and the error was within ± 0.01 s. The typical time for the solvent (distilled water) was 120 s.

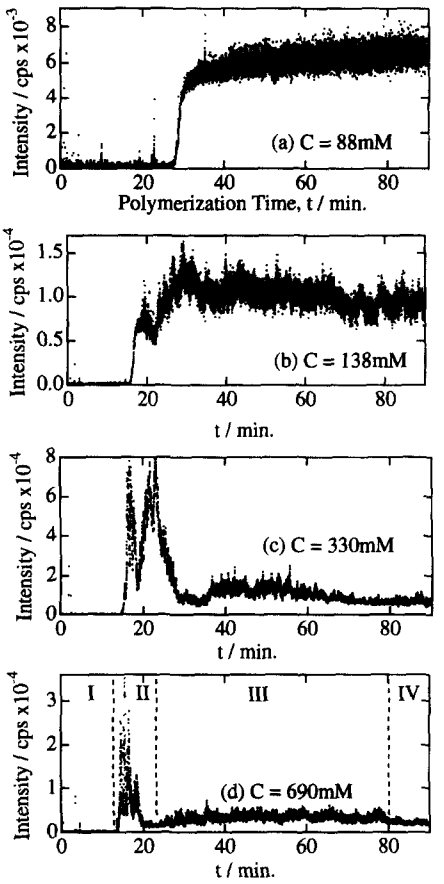

Figure 1 Time evolution of the scattered intensity for PNIPA gels; (a) 88, (b) 138, (c) 330, and (d) 690 mM. (I) the induction stage, (II) the gelation threshold stage, (III) the strong fluctuation stage, and (IV) the plateau stage are denoted in (d)

RESULTS AND DISCUSSION

Time-resolved light scattering

Figure 1 shows the time evolution of the scattered intensity at 60° during the polymerization process of gels with NIPA initial concentrations, C, of (a) 88, (b) 138, (c) 330, and (d) 690 mM. The intensity is quite low at $t <$ 20 min, and then increases stepwise at the threshold polymerization time, $t_{th} \approx$ 20 min. For $C \leq$ 88 mM, the intensity reaches a plateau value and remains rather constant. In this case, no gelation took place, indicating that the concentration was too low to form an infinite cluster. However, for $C \geq$ 330 mM, the intensity increase is abrupt, followed by a gradual decrease with strong fluctuations. Then, finally the intensity levels off with fewer fluctuations. Therefore, we classify the intensity variation with time to four stages characterized by: (I) the induction stage ($t \leq$ 20 min), (II) gelation threshold stage ($t \approx$ 20 min), (III) the strong fluctuation stage (20 $\leq t <$ 80 min), and (IV) the plateau stage (80 min $\leq t$) as depicted in *Figure 1d*. The physical meaning of these stages will be discussed later. A similar phenomenon is also observed in the polymerization process of PNIPA solutions as shown in *Figure 2*, although stage II corresponds to the polymerization period and stage III is absent. A stepwise increase in intensity takes place at $t_{th} \approx$ 20 min, followed by a gradual decrease in intensity. However, there are at least two characteristic features in the time evolution of the scattered intensity for the NIPA polymer solutions. One is that the peak and plateau intensities are significantly lower than those of the gels. The other is that the fluctuations in the

plateau region are rather small compared to those of the gels. The pulses in the plateau region in *Figure 2c* are due to accidental scattering by large clusters or dust and are nothing to do with the gelation process. The intensity fluctuations observed in gels are now known to be the result of the non-ergodicity of gels[21–25] or, more rigourlously speaking, "restricted ergodicity"[26,27]. It is rather surprising that t_{th} is insensitive to the architecture of the polymer, i.e. linear (without BIS) or branched (with BIS), or to the monomer concentration C.

Figure 3 shows the intensity variations of the scattered light, i.e. speckle patterns, for (a) PNIPA gels and (b) PNIPA solutions. Although the polymer concentration was the same, $C = 690$ mM, in both cases, the speckle pattern is much stronger in the gel than in the solution. This is due to the presence of the frozen-in inhomogeneity in the gel. Note that the intensity level of the speckle in the gel is much lower than the peak intensity in the polymerization/cross-linking process shown in *Figure 1*. Therefore, it is obvious that the strong peak in the gelation process has a different origin from the commonly observed speckle in a gel.

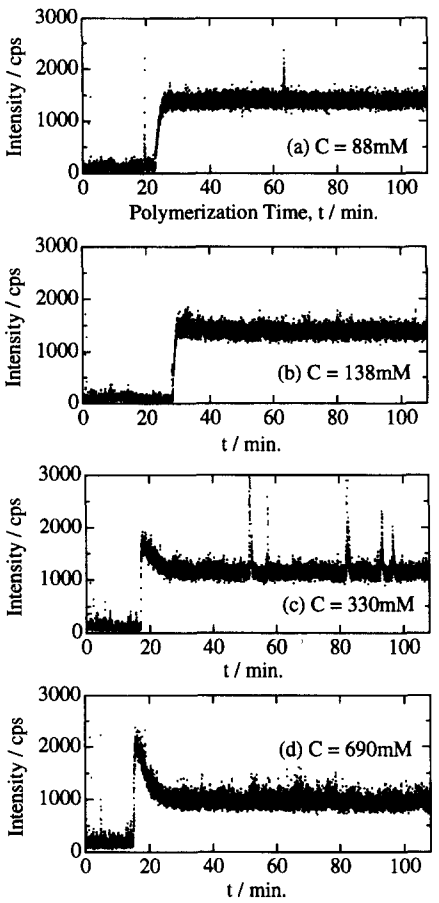

Figure 2 Time evolution of the scattered intensity for PNIPA polymer solutions; (a) 88, (b) 138, (c) 330, and (d) 690 mM

In order to analyse the structure of growing PNIPA chains and/or PNIPA clusters, it is necessary to obtain the q-dependence of the scattered intensity, where q is the magnitude of the scattering vector. Instead, we measured the scattered intensity evolution with time at various angles, namely 45°, 75°, 60° and 90°, and found that the profile of the scattered intensity variation is insensitive to the scattering angle, indicating that chain growth takes place in a very limited time range around $t \approx t_{th}$.

Figure 4 shows the initiator (APS) concentration dependence of the time evolution of the scattered intensity for PNIPA solutions with $C = 690$ mM. The APS concentrations, C_{APS}, were (a) 1.75 mM and (b) 3.50 mM. By doubling the APS concentration, the t_{th} became smaller. This indicates that this intensity rise is related to the concentration of the redox radicals. Though more quantitative investigations were tried to determine t_{th} as a function of APS concentration, it was found that t_{th} was too sensitive to the oxygen in the system to reproduce quantitative results. Note that t_{th} seems to depend on C_{APS} but not strongly on C (see *Figure 1* and *Figure 2*). This suggests that the length of the induction period, i.e. the stage for $t \leq t_{th}$, depends on the concentration of APS radicals.

Figure 5 shows the temperature variation during the polymerization (filled circles; left axis) as well as the scattered intensity (dots; right axis) for (a) gels and (b) polymer solutions. The temperature was measured by setting a thermocouple in the reacting bath. This figure clearly shows that a reaction heat is generated most intensively at the time of the abrupt intensity rise, t_{th}. It should also be noted that this amount of temperature rise does not result in the step-like or abrupt increase in the scattered intensity even though the solubility of PNIPA in water is strongly temperature-dependent[23]. A similar intensity rise was also observed in temperature-insensitive gels, e.g. poly(acrylamide) gels.

Now we characterize the intensity evolution of PNIPA gels and solutions by considering the peak intensity, I_{peak},

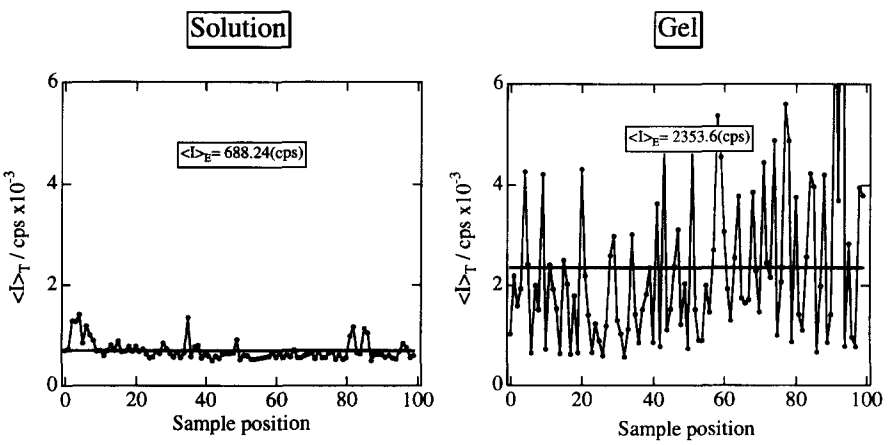

Figure 3 Light-scattered intensity variation with position, i.e. speckle patterns, for (a) PNIPA solution ($C = 690$ mM) and (b) PNIPA gel ($C = 690$ mM). The horizontal line indicates the ensemble average of the scattered intensity, $< I >_E$

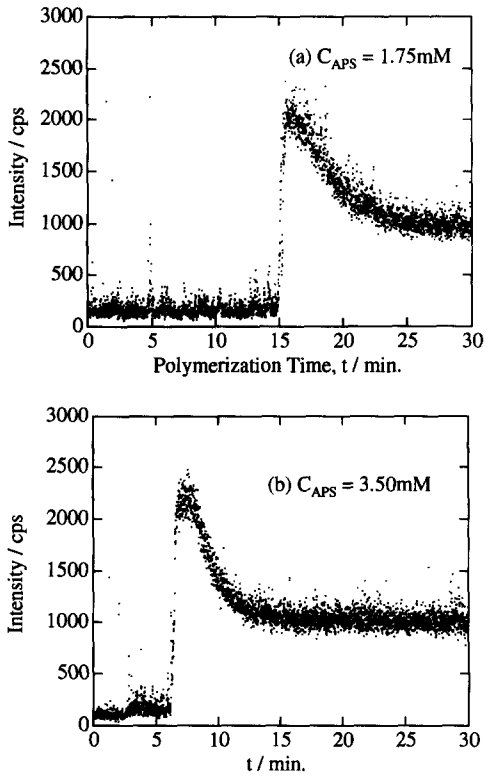

Figure 4 Initiator (APS) concentration dependence of time evolution of the scattered intensity for PNIPA solutions of $C = 690$ mM

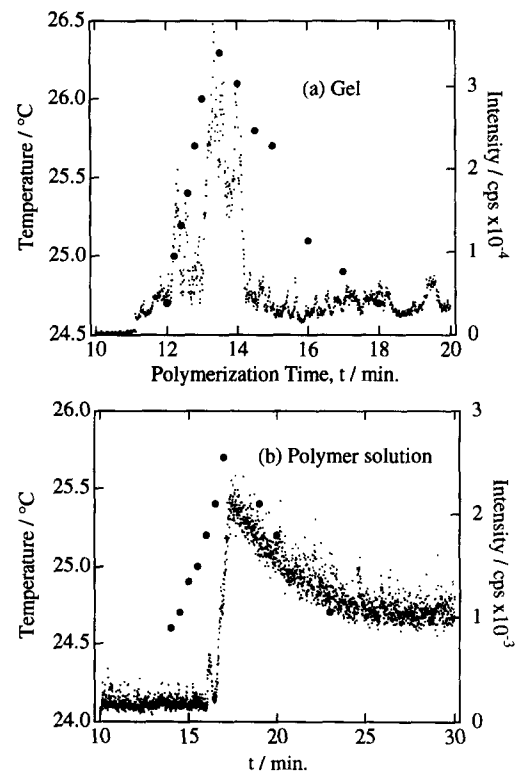

Figure 5 Temperature variation (filled circles) of (a) the PNIPA gels and (b) the polymer solutions. Scattered intensity variation (dots) is indicated on the right axis

and the plateau intensity, $I_{plateau}$, determined by taking an average of the scattered intensities in the plateau region. *Figure 6* shows the C dependence of I_{peak} and $I_{plateau}$ for PNIPA solutions. For $C \geq 138$ mM, I_{peak} deviates from $I_{plateau}$ because of the appearance of the abrupt intensity rise.

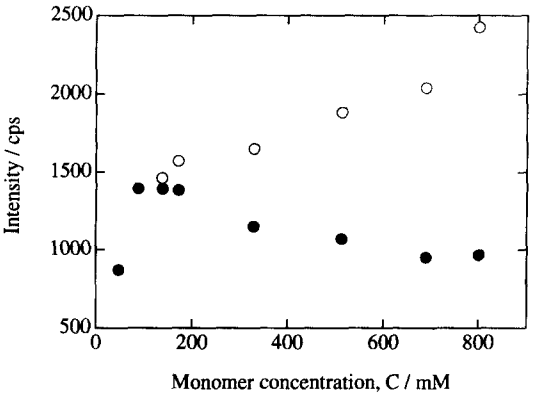

Figure 6 Monomer concentration dependence of the peak, I_{peak} (○), and plateau intensities, $I_{plateau}$ (●), of PNIPA solutions

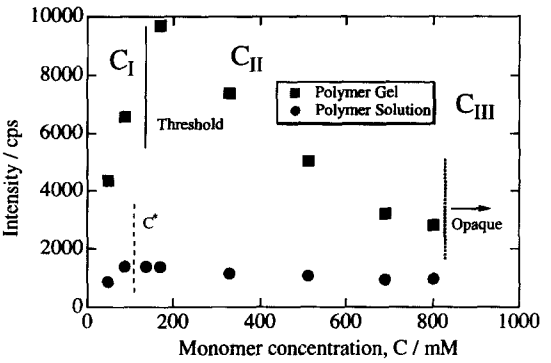

Figure 7 The plateau intensity, $I_{plateau}$ intensity evolution of PNIPA gels and solutions

Interestingly, I_{peak} increases with C while $I_{plateau}$ decreases with increasing C. The increase in I_{peak} with C may be due to the formation of more concentrated clusters at the chain overlap threshold for a solution with a higher C, leading to a larger contrast between the cluster and the solvent. On the other hand, the decrease in $I_{plateau}$ is explained by suppression of concentration fluctuations in the semi-dilute regime for a higher C. Analysis on I_{peak} for PNIPA gels was not carried out because I_{peak} could not be specified due to the appearance of multi-peaks and because the values were not reproducible.

Figure 7 shows $I_{plateau}$ of PNIPA gels and solutions as a function of C. The scattering behaviour of PNIPA gel (marked with closed squares) can be classified into three regimes; (C_I) the finite cluster regime ($C \leq 88$ mM), (C_{II}) the gel regime ($88 < C \leq 801$ mM), and (C_{III}) the phase-separated gel regime ($C > 801$ mM). For convenience, we apply the same classification to the PNIPA solutions (closed circles). In regime C_I, the intensity increases stepwise with time (See *Figure 1a*). This tendency is also observed in PNIPA solutions (See *Figure 2a*). Regime C_{II} is characterized by the appearance of the abrupt increase as shown in *Figure 1c* and *d* and *Figure 2c* and *d*. In this regime, $I_{plateau}$ is a strong function of C. As shown in the figure, $I_{plateau}$ for gels is highest around $C = 171$ mM and decreases with C. This concentration may correspond to the chain overlap concentration, C^*, as will be discussed in conjunction with the results of the viscosity measurement. The decrease in $I_{plateau}$ with C indicates suppression of the concentration fluctuations. However, $I_{plateau}$ is much stronger for the gels than for the polymer solutions. This is due to the presence of frozen inhomogeneity in gels introduced by cross-link formation. This aspect is extensively studied elsewhere[24]. In this

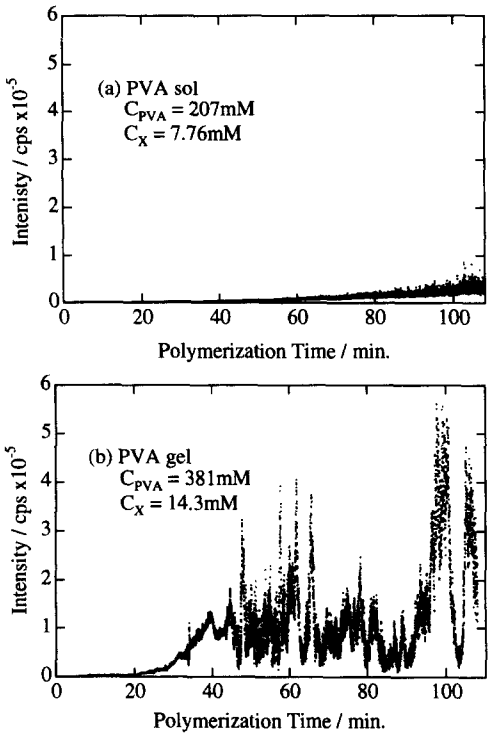

Figure 8 Time evolution of the scattered intensity for (a) poly(vinyl alcohol) (PVA) sol (C_{PVA} = 207 mM, C_X = 7.7 mM), and (b) PVA gel (C_{PVA} = 381 mM, C_X = 14.3 mM) cross-linked with glutaraldehyde

regime, the so-called gel mode is observed. That is, a single-exponential time intensity correlation function is obtained from which the collective diffusion coefficient is evaluated[25]. In regime C_{III}, however, the monomer concentration is too high as a gel, resulting in a phase separation. This was confirmed by the fact that the gel became opaque. Such a phase separation was not observed in PNIPA solutions even for $C > 801$ mM. This clearly shows that a cross-link formation is the same as an increase in the attractive interaction and leads to segregation, as pointed out by de Gennes[12].

In the case of gel formation from a polymer solution by photo-cross-linking, by radiation cross-linking, or by adding a cross-linking agent, this method may not be sensitive enough to detect the onset of gelation because concentration fluctuations already exist in the polymer solution. We examined a case of the chemical cross-linking process of poly(vinyl alcohol) (PVA) aqueous solutions with glutaraldehyde. *Figure 8* shows the results of the time evolution of the scattered intensity for (a) PVA sol (C_{PVA} = 207 mM, C_X = 7.76 mM), and (b) PVA gel (C_{PVA} = 381 mM, C_X = 14.3 mM), where C_{PVA} and C_X are the PVA concentration in the monomer unit and the cross-linking agent concentration, respectively. Gelation was not observed for the former while a steady gel was formed in the case of (b). Although the scattered intensity increases with time in both cases, that for the PVA gel is much more pronounced. In addition, strong intensity fluctuations appear for the PVA gel at $t >$ 40 min. The behaviour in the gel is very similar to the case of PNIPA gel, except for the absence of the abrupt intensity rise. Thus, it can be deduced that TRLS reveals gel formation as strong intensity fluctuations and the appearance of a speckle pattern at $t > 40$ min. Therefore, by comparing *Figure 1* and *Figure 8*, it may be concluded that TRLS is a sensitive technique to detect gelation processes of both types, i.e. gelation/polymerization and cross-linking of

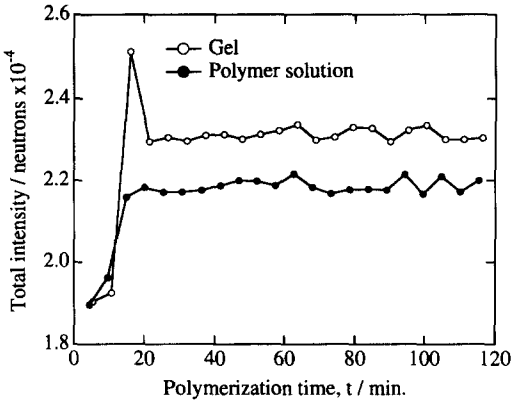

Figure 9 The t dependence of the total scattered intensity obtained by small-angle neutron scattering (SANS)

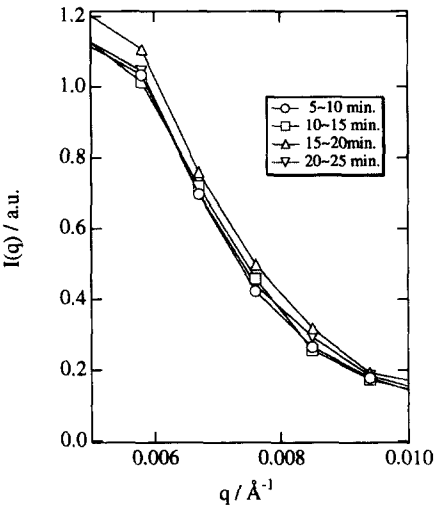

Figure 10 The scattered intensity profile, $I(q)$, for PNIPA gels, obtained at different t's

a polymer solution, and is particularly useful in studies of the former.

SANS

Figure 9 shows the t dependence of the total scattered intensity obtained by small-angle neutron scattering (SANS) for the range of $0.005 \leq q \leq 0.08$ Å^{-1}. Because of a lack of statistical accuracy, the total intensities collected with an area detector for every 5 min period are plotted as a function of t after subtraction of the solvent scattering. Interestingly, an abrupt intensity rise was observed exclusively in the gel sample (C = 690 mM), followed by a levelling off to a plateau intensity. *Figure 10* shows the scattered intensity profile, $I(q)$, for PNIPA gels obtained at different t's. The lines connecting the data are drawn for the eye. Unlike the total intensity, $I(q)$ does not seem to be sensitive to the gelation or cluster formation although an increase in $I(q)$ is detected for $q \leq 0.01$ Å^{-1} during the period of $15 < t \leq 20$ min. Note that the difference in the q range; $q \approx 0.001$ Å^{-1} (TRLS) and $0.005 \leq q \leq 0.01$ Å^{-1} (SANS). It is clear from *Figure 1* and *Figure 10* that TRLS is a more relevant method than SANS for investigating gelation kinetics. This is due to the fact that SANS is sensitive to the concentration fluctuations inside a cluster of which the length scale is much smaller than the cluster size near the gelation threshold. On the other hand, TRLS is sensitive to large clusters of the order of micrometers, with

the result that TRLS can be a sensitive tool for the detection of the gelation threshold. It should be stressed here, however, that the observed SANS intensity was too low, because of the short counting time (5 min), to analyse the gelation process quantitatively and that the concentration fluctuations by cross-linking are also detectable by SANS.

Viscometry and chain overlap concentration

In order to elucidate the physical significance of the abrupt intensity rise in the TRLS, viscosity measurements were conducted. *Figure 11* shows the reduced viscosity, η_{sp}/C, as a function of the polymer concentration in monomeric units, C. A PNIPA solution made from a 88 mM monomer solution was diluted and used for the viscosity measurement. As shown in the figure, the data points roughly fall on a straight line, from which the intrinsic viscosity, $[\eta]$, was estimated to be 8.96×10^{-2} cm^3 g^{-1} at 25°C. The intrinsic viscosity is related to the ratio of the mean-square radius of gyration, $< S^2 >$, and the molecular mass, M, as follows

$$[\eta] = 6^{3/2}\Phi[< S^2 >]^{3/2}/M \quad (1)$$

where Φ is the Flory universal constant[3]. The chain overlap concentration, C^*, on the other hand, is given by letting the average concentration in the volume occupied by a single chain be equal to the average monomer concentration

$$C^* = \frac{3M}{4\pi N_A[< S^2 >]^{3/2}} \quad (2)$$

where N_A is Avogadro's number. By substituting equation (1) into equation (2), one obtains

$$C^* = \frac{3 \times 6^{3/2}\Phi}{4\pi N_A[\eta]} \quad (3)$$

The value of Φ is known to be $2.3\sim2.8 \times 10^{23}$ for dilute polymer solutions at the Θ condition and is independent of the molecular mass[28]. According to Kubota et al., $\Theta = 30.5$°C is reported for a PNIPA solution of $M = 9.10 \times 10^6$[29]. In the case of a good solvent system, Φ is a decreasing function of molecular weight[28]. However, as an approximation, one can assume the invariance of Φ with respect to M. We employed $\Phi = 2.1 \times 10^{23}$ for the value of a polydisperse system and obtained $C^* = 109.7$ mM at 25°C. This concentration is reasonably close to the one at which the abrupt intensity rise starts to appear in both the gel and solution cases, i.e., $C^* \approx 88$ mM. Therefore, we believe that the stepwise increase in the scattered intensity corresponds to the chain overlapping threshold (for the case of polymer solutions). This finding does not directly mean that the abrupt intensity rise in gels observed in *Figure 1* indicates the gelation threshold. However, since t_{th} is not sensitive to the chemical structure and I_{peak} has a peak at $C = 171$ mM for the gel (*Figure 7*), it can be approximated that the abrupt increase also corresponds to the gelation threshold. Note that the concentration fluctuations are expected to be largest at the gelation threshold. Therefore, it can be concluded that time-resolved light scattering is a sensitive tool for the detection of the gelation threshold.

Gelation model

Figure 12 is a schemetic representation of the gel formation process as a function of polymerization time, t. The observed phenomena can be described as follows: For $t < t_{th}$ (stage I), no intensity rise is observed. This is the induction period and polymerization of NIPA does not take place. Therefore the system remains as a monomer solution.

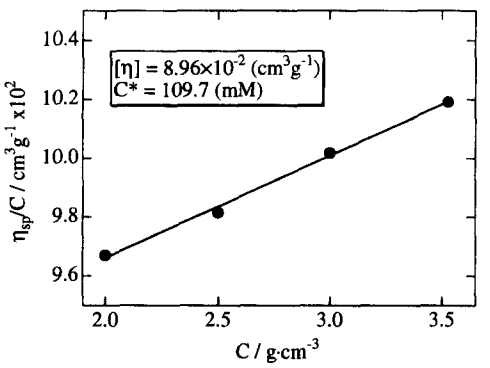

Figure 11 The reduced viscosity, η_{sp}/C, as a function of the polymer concentration in monomeric units, C

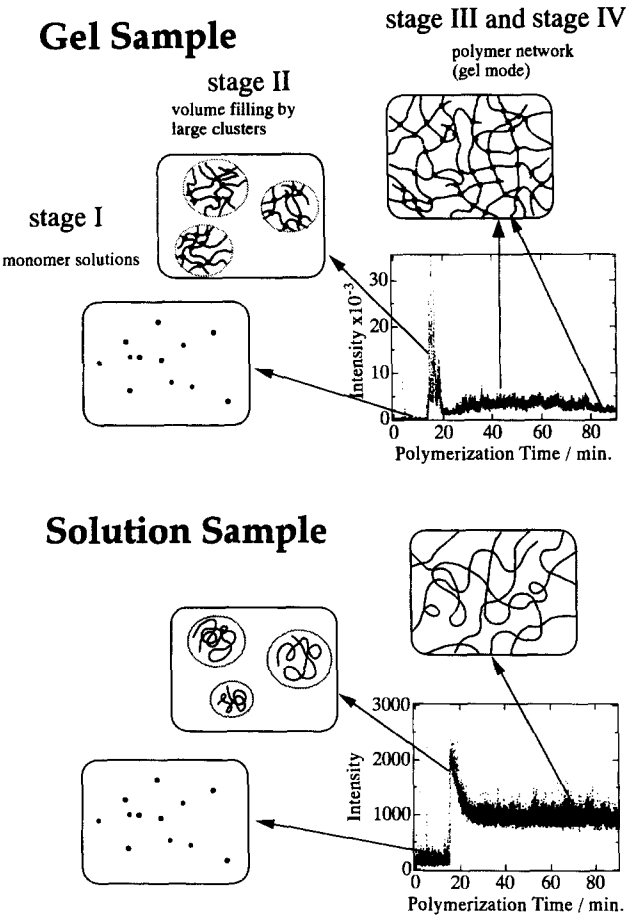

Figure 12 Schematic model of the gel formation process against the polymerization time, t. In stage I, only monomer solutions are present where the monomers are represented as dots. In stage II, PNIPA clusters (gel) or chains (solution) of finite sizes indicated by lines and circles are formed, which eventually fill the volume. This stage is followed by stage III where permanent (gel) or entangled networks (solution) are created and the thermal fluctuations are dominated by local concentration fluctuations within the blobs

Polymerization occurs suddenly at t_{th} and the size of PNIPA clusters (or chains) becomes large and detectable by light scattering at $t > t_{th}$. Thus, an abrupt intensity rise is observed by approaching the volume-filling threshold dominated by infinite clusters (for the gels) or by overlapping polymer chains (for the linear polymers) (stage II). After the volume filling, the scattering is ascribed not to cluster scattering (or individual polymer scattering) but to the thermal fluctuations and frozen inhomogeneity of the network. Since the characteristic size of the network is the

mesh size and is much smaller than the cluster size (or individual polymer size), the scattered intensity is gradually suppressed compared to the peak intensity although the gelation/polymerization reaction continues and a related rearrangement of chain conformation takes place (the strong fluctuation stage, III). This stage is followed by a steady state after completion of the reaction (the plateau stage, IV). The fluctuations of the scattered intensity for gels in stage IV are due to the frozen inhomogeneity and thermal fluctuations. In this stage, the scattered intensity can be decomposed into the time-fluctuating (dynamic) part and the position-dependent (static or frozen) part. We have verified that the dynamic part is essentially the same as the fluctuations observed in the corresponding polymer solutions with the same concentration as reported elsewhere[21]. A further investigation of the gelation/polymerization kinetics is now in progress in terms of electron spin resonance.

CONCLUSION

Time-resolved light scattering has been employed to study the gelation/polymerization kinetics of poly(*N*-isopropyl acrylamide) (PNIPA) gels and solutions. The scattered intensity increased suddenly at the threshold time, $t_{th} \approx 20$ min after the polymerization was initiated. When the monomer concentration was higher than the so-called chain overlap concentration, C^*, the intensity rise became abrupt, followed by a gradual decrease to a plateau value. The time course of the scattered intensity variation for the PNIPA gels can be classified into four regimes: (I) the induction stage, (II) the gelation threshold stage, (III) the strong fluctuation stage, and (IV) the plateau stage. A clear difference in the scattering behaviour between the PNIPA gels and the corresponding polymer solutions was also observed. Firstly, the peak intensity of the gel is much higher than that of the solution. Secondly, the strong fluctuation stage is only present for the gels before entering the plateau regime, $I_{plateau}$. Thirdly, $I_{plateau}$ for the gels is much larger than that for the polymer solution. These characteristic features of the scattering from gels are due to the presence of spatial inhomogeneity introduced by cross-link formation. It is concluded that both the gelation threshold, t_{th}, and the chain overlap concentration, C^*, can be determined by time-resolved light scattering experiments during the polymerization/gelation process on a series of pre-gel solutions with different monomer concentrations.

ACKNOWLEDGEMENTS

This work is supported by the Ministry of Education, Science, Sports and Culture, Japan (Grant-in-Aid, No. 08231245 and 09450362 to M. S.). This work was performed with the approval of Solid State Physics Laboratory, The University of Tokyo (Proposal No. 6749), at Japan Atomic Energy Research Institute, Tokai, Japan.

REFERENCES

1. Flory, P. J., *J. Am. Chem. Soc.*, 1941, **63**, 3038.
2. Flory, P. J., *Chem. Revs.*, 1946, **39**, 137.
3. Flory, P. J., *Principles of Polymer Chemistry*, Cornell Univ. Press, 1953.
4. Stockmayer, W., *J. Chem. Phys.*, 1943, **11**, 45.
5. Stockmayer, W., *J. Chem. Phys.*, 1944, **12**, 125.
6. Stauffer, D., *Phys. Report*, 1979, **54**, 1.
7. Stauffer, D., Coniglio, A. and Adam, M., *Adv. Polym. Sci.*, 1982, **44**, 103.
8. Schmidt, W. and Burchard, W., *Macromolecules*, 1981, **14**, 370.
9. Adam, M., Delsanti, M., Munch, J. P. and Durand, D., *J. Physique*, 1987, **48**, 1809.
10. Martin, J. E. and Wilconxon, J. P., *Phys. Rev.*, 1989, **A39**, 352.
11. Bouchaud, E., Delsanti, M., Adam, M., Daoud, M. and Durand, D., *J. Physique*, 1986, **47**, 1273.
12. de Gennes, P. G., *Scaling Concepts in Polymer Physics*, Cornell Univ. Press, 1979.
13. Chambon, F. and Winter, H. H., *Polym. Bull.*, 1985, **13**, 499.
14. Winter, H. H. and Chambon, F., *J. Rheol.*, 1986, **30**, 367.
15. Chambon, F., Petrovic, Z. S., MacKnight, W. J. and Winter, H. H., *Macromolecules*, 1986, **19**, 2146.
16. Kobayasi, S., *Rev. Sci. Instrum.*, 1985, **56**, 160.
17. Allain, C., Drifford, M. and Gauthier-Manuel, B., *Polymer*, 1986, **27**, 177.
18. Wu, C., Zuo, J. and Chu, B., *Macromolecules*, 1989, **22**, 838.
19. Fang, L., Brown, W. and Knoak, C., *Macromolecules*, 1991, **24**, 6839.
20. Ikkai, F., Shibayama, M., Momura, S. and Han, C. C., *J. Polym. Sci., Polym. Phys. Ed.*, 1996, **34**, 939.
21. Pusey, P. N. and van Megen, W., *Physica A*, 1989, **157**, 705.
22. Joosten, J. G.H., McCarthy, J. L. and Pusey, P. N., *Macromolecules*, 1991, **24**, 6690.
23. Shibayama, M., Fujikawa, Y. and Nomura, S., *Macromolecules*, 1996, **29**, 6535.
24. Shibayama, M., Norisuye, T. and Nomura, S., *Macromolecules*, 1996, **29**, 8746.
25. Tanaka, T., Hocker, L. O. and Benedek, G. B., *J. Chem. Phys.*, 1973, **59**, 5151.
26. Panyukov, S. and Rabin, Y., *Phys. Report*, 1996, **269**, 1.
27. Shibayama, M., *Macromol. Chem. Phys.*, in press.
28. Fujita, H., *Polymer Solution*, Elsevier, Amsterdam, 1990.
29. Kubota, K., Fujishige, S. and Ando, I., *Polym. J.*, 1990, **22**, 15.